LCAT deficiency does not impair amyloid metabolism in APP/PS1 mice[S]

Sophie Stukas,* Lita Freeman,† Michael Lee,* Anna Wilkinson,* Alice Ossoli,† Boris Vaisman,† Stephen Demosky,† Jeniffer Chan,* Veronica Hirsch-Reinshagen,* Alan T. Remaley,† and Cheryl L. Wellington[1],*

Department of Pathology and Laboratory Medicine,* Child and Family Research Institute, University of British Columbia, Vancouver, British Columbia, Canada V5Z 4H4; and National Institutes of Health,† Bethesda, MD 20892-1508

Abstract **A key step in plasma HDL maturation from discoidal to spherical particles is the esterification of cholesterol to cholesteryl ester, which is catalyzed by LCAT. HDL-like lipoproteins in cerebrospinal fluid (CSF) are also spherical, whereas nascent lipoprotein particles secreted from astrocytes are discoidal, suggesting that LCAT may play a similar role in the CNS. In plasma, apoA-I is the main LCAT activator, while in the CNS, it is believed to be apoE. apoE is directly involved in the pathological progression of Alzheimer's disease, including facilitating β-amyloid (Aβ) clearance from the brain, a function that requires its lipidation by ABCA1. However, whether apoE particle maturation by LCAT is also required for Aβ clearance is unknown. Here we characterized the impact of LCAT deficiency on CNS lipoprotein metabolism and amyloid pathology. Deletion of LCAT from APP/PS1 mice resulted in a pronounced decrease of apoA-I in plasma that was paralleled by decreased apoA-I levels in CSF and brain tissue, whereas apoE levels were unaffected. Furthermore, LCAT deficiency did not increase Aβ or amyloid in APP/PS1 LCAT$^{-/-}$ mice. Finally, LCAT expression and plasma activity were unaffected by age or the onset of Alzheimer's-like pathology in APP/PS1 mice. Taken together, these results suggest that apoE-containing discoidal HDLs do not require LCAT-dependent maturation to mediate efficient Aβ clearance.**—Stukas, S., L. Freeman, M. Lee, A. Wilkinson, A. Ossoli, B. Vaisman, S. Demosky, J. Chan, V. Hirsch-Reinshagen, A. T. Remaley, and C. L. Wellington. **LCAT deficiency does not impair amyloid metabolism in APP/PS1 mice.** ***J. Lipid Res.*** **2014.** 55: **1721–1729.**

Supplementary key words lecithin:cholesterol acyltransferase • high density lipoprotein metabolism • apolipoproteins • Alzheimer's disease

Lipoprotein metabolism in the CNS is intimately involved in the progression and pathogenesis of Alzheimer's disease (AD) (1). Since the 1993 discovery that inheritance of the apoE4 allele increases risk and decreases the age of onset of late-onset AD (2), the putative roles of apoE in AD pathogenesis have been a topic of intensive focus. apoE is the primary apolipoprotein secreted by astrocytes and microglia in the CNS, and lipidation of nascent apoE-containing discoidal particles eventually leads to the formation of mature CNS HDL-like particles in cerebrospinal fluid (CSF) (1, 3).

It is well-established that amyloid burden in humans follows an isoform-dependent pattern of apoE4>apoE3>apoE2 (4–6). In contrast to human apoE, murine apoE exists in only one isoform with limited homology to human apoE. Amyloid burden is robust in AD mice expressing murine apoE and nearly abrogated in apoE-deficient mice (7–11). Reconstitution of human apoE isoforms into AD mice greatly delays amyloid deposition relative to murine apoE, but retains the human isoform-specific influence on amyloid accumulation (12–17). Taken together, the relative amyloid burden across murine and human apoE is: murine apoE>>apoE4>apoE3>apoE2>>apoE$^{-/-}$. These observations clearly show that apoE affects amyloid burden in vivo.

In vivo, neither apoE isoform nor gene dose significantly affects the rate of β-amyloid (Aβ) production from amyloid precursor protein (16, 17), leading to the consensus that apoE is largely involved in modulating the clearance of Aβ peptides from the brain. apoE participates in each of the three known pathways of Aβ clearance, including proteolytic degradation, egress across the blood-brain barrier, and interstitial fluid drainage, although many details remain poorly understood (18, 19). It is important to note, however, that apoE isoforms, levels, and lipidation status are all important variables.

This work was supported by operating grants from the Heart and Stroke Foundation of Canada and the Canadian Institutes of Health Research (CIHR) to C.L.W., a CIHR Vanier Scholarship to S.S., and a CIHR postdoctoral fellowship to V.H-R. A.T.R., L.F., A.O., and B.V. were supported by intramural National Heart, Lung, and Blood Institute research funds.

Manuscript received 5 April 2014 and in revised form 12 June 2014.

Published, JLR Papers in Press, June 20, 2014
DOI 10.1194/jlr.M049940

Abbreviations: AD, Alzheimer's disease; Aβ, β-amyloid; CE, cholesteryl ester; CIHR, Canadian Institutes of Health Research; CSF, cerebrospinal fluid; FC, free cholesterol; GuHCl, guanidine hydrochloride; HDL-C, HDL cholesterol; LDLR, LDL receptor; LRP1, LDL receptor-related protein 1.

[1]To whom correspondence should be addressed.
e-mail: Cheryl@cmmt.ubc.ca

[S] The online version of this article (available at http://www.jlr.org) contains supplementary data in the form of two figures and text.

With respect to apoE levels, most studies suggest that apoE promotes retention of Aβ in the brain, as brain-to-blood transport of radiolabeled Aβ injected into the brain is slowed when premixed with human apoE compared with free Aβ (20, 21). Also supporting this viewpoint is the observation that amyloid burden is lower in hemizygous APOE3 and APOE4 APP/PS1-21 and hAPP J20 AD mice compared with homozygous controls (17, 22). Intriguingly, as a recent microdialysis study showed that very little apoE is actually associated with soluble Aβ in brain interstitial fluid, apoE may retard Aβ clearance from brain to blood by competing with Aβ for binding to the LDL receptor-related protein 1 (LRP1) (23). However, another study found that there was significant interaction between apoE and Aβ, and that the levels of soluble apoE-Aβ decreased in an isoform-specific manner apoE4<apoE3<apoE2 (24). These observations suggest that the putative interactions between apoE and Aβ may vary depending on the experimental conditions and pools of apoE and Aβ that are studied. Additionally, brain-specific overexpression of the LDL receptor (LDLR), the major apoE receptor (25), leads to significantly decreased brain apoE levels and significantly reduced amyloid and Aβ loads, presumably by accelerating apoE uptake (26, 27).

How apoE is involved in Aβ metabolism is not completely understood, as net levels of apoE are only one part of the equation; the degree to which apoE is lipidated also significantly affects function. Lipidation of apoE in the CNS is performed by ABCA1 (28, 29), akin to the well-established role of ABCA1-mediated lipidation of apoA-I in the periphery (30). Plasma and CSF apoA-I levels are markedly reduced in mice deficient in ABCA1, whereas CSF and brain tissue apoE are decreased by 60–80% (28, 29, 31). ABCA1$^{-/-}$ mice display increased insoluble Aβ and amyloid deposition when crossed onto the TgSwDI (32), APP23 (33), and PDAPP (34) mouse models of AD. Conversely, selective overexpression of ABCA1 by 6-fold or more is sufficient to prevent the formation of amyloid plaques without altering the net levels of CNS apoE or apoA-I in PDAPP mice (35).

Similar to apoA-I-containing HDL particles in plasma, apoE-containing HDL-like particles in the CNS exist in two major structural conformations depending on their maturation state (3). In vitro, astrocytes, and to a lesser extent, microglia, secrete several nascent discoidal apoE particles ranging from 7.5 to 17 nm in diameter that contain 0–18% of their cholesterol as esters (36–39). By contrast, apoE- and apoA-I-containing lipoprotein particles in CSF are 11–20 nm spherical particles containing 70% of their cholesterol in the esterified form, with a similar density to α-HDL found in plasma (38, 40–42). Plasma HDL maturation is catalyzed by LCAT, which esterifies free cholesterol (FC) to cholesteryl ester (CE) to form the lipid core critical for conversion of discoidal preβ-HDL to mature spherical α-HDL (43). In addition to HDL, LCAT can also esterify FC contained on other lipoprotein particles, thus influencing their metabolism as well. In plasma, HDL maturation maintains the gradient of FC between the cell membrane and HDL surface, thereby driving cholesterol efflux, a key process in reverse cholesterol transport (43). Plasma α-HDL and apoA-I levels are dramatically reduced in LCAT$^{-/-}$ mice (44, 45), however the macrophage reverse cholesterol transport pathway is largely preserved (46). Whether LCAT is pro- or antiatherogenic remains contested, as results from both animal and human studies are conflicting (43).

In the CNS, we have previously shown that LCAT is secreted by astrocytes and is capable of esterifying FC contained on glial-derived nascent apoE-containing particles (47). apoE is hypothesized to be the major LCAT activator in the CNS, as apoE is sufficient to stimulate esterification of endogenous cholesterol in glial-conditioned media (39). apoA-I, which is not synthesized within the CNS but is found in CSF, is also capable of esterifying cholesterol using glial-derived LCAT (47). The levels and activity of LCAT in CSF are estimated to be 2.2–2.5% of serum LCAT (42, 48). In young C57Bl.6 mice, LCAT deficiency leads to a dramatic increase in apoE and a concurrent decrease of apoA-I levels in CSF (47), suggesting that LCAT activity may in part regulate CSF apoE and apoA-I levels.

LCAT activity in the CSF of AD subjects has been reported to be up to 50% lower than in cognitively normal subjects (42). It is not known whether this association may be related to Aβ metabolism, such that reduced LCAT may impair Aβ clearance. It is also not known whether aging or the presence of Aβ may impair LCAT activity. To address the question of whether Aβ clearance requires LCAT-mediated maturation of apoE-bearing HDL-like particles, we assessed the impact of LCAT deficiency on soluble and aggregated Aβ levels as well as parenchymal and vascular amyloid burden in the APP/PS1 model of AD. We also assessed the impact of aging and Aβ accumulation on LCAT expression and activity. Here we report that protein levels and plasma activity of LCAT are not altered by age and/or Aβ accumulation and that neither Aβ nor amyloid levels are increased in the absence of LCAT. We conclude that LCAT-mediated cholesterol esterification and maturation of apoE-containing lipoproteins in the CNS is not required for apoE's role in Aβ metabolism.

MATERIALS AND METHODS

Animals

APP/PS1 (line 85) mice (Jackson Laboratories), which coexpress two transgenes from the murine prion promoter: a chimeric mouse/human APP cDNA containing the Swedish (K670M/N671L) mutations and the human PS1 gene deleted for exon 9, were crossed with LCAT$^{-/-}$ animals followed by one backcross to generate male APP/PS1 LCAT$^{-/-}$ mice. Male APP/PS1 mice were analyzed at 15–16 months of age, unless otherwise stated. Animals were maintained on a standard chow diet (PMI LabDiet 5010). All procedures involving experimental animals were approved by the Canadian Council of Animal Care and the University of British Columbia Committee on Animal Care.

CSF, plasma, and tissue collection

Mice were anesthetized by intraperitoneal administration of a mixture of 20 mg/kg xylazine (Bayer) and 150 mg/kg ketamine

(Bimeda-MTC). CSF was isolated from the cisterna magna as described (49). Blood was collected via cardiac puncture, placed into tubes containing EDTA, and centrifuged at 21,000 rcf for 10 min and stored at −80°C until use. Animals were then perfused for 7 min at 8 ml/min with PBS containing 2,500 U/l heparin. Liver and brain were extracted and the cortex and hippocampus were dissected and snap-frozen separately at −80°C. Half of the brain was placed into 10% neutral buffered formalin followed by 30% sucrose in PBS for histological analysis.

Plasma lipid and lipoprotein analysis

Plasma HDL cholesterol (HDL-C) was determined using commercially available kits (Wako Diagnostics) according to the manufacturer's instructions. Plasma lipoprotein species were further analyzed by separating them based on size and charge and staining for lipids using Sudan Black. Hydragel 15 Lipoprotein(E) kits (Sebia, 4134) were purchased from Sebia, Inc. Neat plasma (10 μl) was loaded into each well of the applicator and left at room temperature for 5 min. A Hydragel 15 Lipoprotein(E) gel was quickly blotted with thin filter paper to absorb excess liquid on the surface of the gel according to manufacturer's instructions. After the 5 min loading period, the applicator was placed perpendicular to the Hydragel, 3–4 cm from the bottom of the gel. After a 10 min application of sample to the gel, the applicator was removed and the gel was subjected to electrophoresis in 1× barbital buffer (Sigma, B5934-12VL, 1 vial dissolved in 1 l distilled water) in a Titan gel electrophoresis apparatus (Helena Laboratories) with 25 ml barbital buffer per side. The gel was run for 40 min at 100 V using a Bio-Rad PowerPac 100 power supply. After the run, the gel was placed in fixing solution (3% methanol, 57% ethanol, and 10% glacial acetic acid in distilled water) for 10 min. The gel was then dried in a 60°C oven (3 h to overnight), incubated in staining solution (54% ethanol in distilled water containing 200 μl Sudan black per 40 ml final volume) for 10–15 min, destained in discoloring solution (45% ethanol in distilled water) for 5 min, and then dried in a 60°C oven for 10 min.

Plasma LCAT activity assay

LCAT activity in plasma was assayed as described previously (50) with modifications (51). Briefly, artificial substrate for LCAT, [1,2-^{3}H(N)]cholesterol (Perkin Elmer, NET139001MC) labeled liposomes were prepared as described (51). Each plasma sample was analyzed in triplicate using 2 μl per measurement. Tubes with 60 μl of labeled liposomes and 2 μl of plasma were incubated for 30 min at 37°C, after which the reaction was stopped by 1 ml of cold ethanol. Tubes were kept at −20°C for 2–12 h and then centrifuged at 13,000 *g* for 10 min at 4°C. The supernatant was evaporated in a SpeedVac and then dissolved in 30 μl of chloroform with addition of unlabeled cholesterol and CE markers. The substrate and product of the LCAT reaction were separated by thin-layer chromatography using flexible silica polyester backed plates (Whatman, 4410221). The FC and cholesteryl oleate spots on the plates were localized by standard staining in the chamber with iodine vapor, then transferred into scintillation vials and counted. The results obtained were used to calculate the coefficient of esterification (ratio CE/FC) and specific LCAT activity in nanomoles per milliliter per hour. In these calculations, the original amount of FC in the reaction was calculated as the cholesterol in liposomes plus FC taken with 2 μl of plasma (52).

Protein extraction

Cortex and hippocampus samples from APP/PS1 WT and LCAT$^{-/-}$ mice were homogenized in 8 volumes of ice-cold carbonate buffer [100 mM Na_2CO_3, 50 mM NaCl (pH 11.5)] containing complete protease inhibitor (Roche Applied Science) in a Tissuemite homogenizer for 20 s, sonicated at 20% output for 10 s, and clarified by centrifugation at 16,600 rcf for 45 min at 4°C. The supernatant (carbonate-soluble fraction) was removed and neutralized by adding approximately 1.5 volumes of 1 M Tris (pH 6.8) to give a final pH of approximately 7.4. The remaining pellet was resuspended in guanidine hydrochloride (GuHCl) extraction buffer [5 M GuHCl, 50 mM Tris HCl (pH 7.4)]. For measurement of LCAT, cortex and liver samples were homogenized in 8 volumes of ice-cold RIPA lysis buffer containing complete protease inhibitor (Roche Applied Science) in a Tissuemite homogenizer for 20 s, sonicated at 20% output for 10 s, and centrifuged at 8,600 rcf for 10 min at 4°C. Protein concentrations were determined using a BCA assay (Pierce).

Immunoblotting

Equal volumes of CSF (5 μl), plasma (1 μl), or tissue lysate (50–75 μg) were electrophoresed through 10% SDS-PAGE, transferred to polyvinyl difluoride membranes (Millipore), probed using a murine-specific apoA-I antibody (1:500 to 1:2,000; Meridian, K23001R), an apoE antibody (1:1,000; Santa Cruz Biotechnology, clone M20, sc-6384), mouse anti-albumin (1:2,000 to 1:5,000; Bethyl Laboratories, A90-134), and mouse anti-GAPDH (1:5,000; Millipore, MAB374) followed by HRP-conjugated secondary antibodies. For LCAT immunoblots, 1.5 μl plasma were electrophoresed through Novex NuPAGE 4–12% Bis-Tris gels (Invitrogen) and proteins were transferred to membranes and probed with LCAT antibodies (Epitomics, 3437) as described previously (53). Blots were developed using enhanced chemiluminescence (Amersham) and quantified by densitometry using ImageJ software (National Institutes of Health). Protein levels were normalized to GAPDH or albumin and expressed as fold difference compared with controls. Each sample was analyzed at least in duplicate on independent gels.

Aβ ELISA

Human $A\beta_{40}$ and $A\beta_{42}$ levels were quantified by commercial ELISA kits (Invitrogen, KMB3482 and KMB3442) following the manufacturer's instructions. Levels of $A\beta_{40}$ and $A\beta_{42}$ were normalized to total protein.

Histology

Five 25 μm sagittal sections spaced approximately 300 μM apart spanning the entire length of the hippocampus were analyzed per animal. Sections were mounted on SuperFrost Plus glass slides (Fisher Scientific), immersed for 10 min in 1% thioflavin S solution, washed with water, and coverslipped using Vectashield Hard Set mounting medium (Vector Laboratories). An additional two sections per mouse were first stained with resorufin, which selectively binds vascular amyloid (54). Sections were washed with PBS, permeabilized for 30 min in PBS containing 0.25% Triton X-100 (PBS-T), stained with 1 μM resorufin in PBS-T for 30 min, followed by three washes in PBS, one wash in 1:1 PBS and ethanol, and three washes in PBS. Sections were then mounted and stained with thioflavin S as described above. Images were taken using a BX61 fluorescent microscope (Olympus) and quantified using Image Pro (Media Cybernetics) software. Amyloid within the area of interest (cortex, hippocampus, thalamus, or cortical vessels) was identified by intensity-level threshold. Amyloid load (defined as the sum of thioflavin S positive area /total area analyzed × 100) was calculated for each section and then averaged across sections for each individual mouse. Total amyloid (parenchymal + vascular) was measured using thioflavin S while vascular amyloid in the cortex was measured using both thioflavin S and resorufin.

mRNA extraction and quantitative RT-PCR

Liver and brain cortex tissue were homogenized in Trizol with a Precellys24 homogenizer and RNA was extracted and purified with a PureLink mini kit followed by quantification using a nanodrop spectrophotometer at 260 nm. Absorbance at 230 and 280 nm was also measured to determine nucleic acid purity. One microgram of RNA was reverse-transcribed in cDNA by TaqMan reverse transcriptase reagents kit (Life Technologies) and 40 ng of cDNA was used for each quantitative PCR reaction. LCAT gene expression in liver and brain cortex was evaluated through real-time PCR assay by the TaqMan method. Mm00500505_m1 probe (Life Technologies) was utilized for LCAT evaluation and β-actin was utilized as housekeeping gene (Life Technologies, 4352341E probe). Data were calculated by the comparative C_T ($\Delta\Delta C_T$) method with normalization of the raw data to β-actin and expressed as fold-change relative to the 5-month-old APP/PS1 mice prior to amyloid deposition.

Statistical analysis

Data were analyzed by either an unpaired two-tailed Student's *t*-test or one-way ANOVA followed by a Bonferroni post hoc test for normally distributed data or a Mann Whitney test or Kruskal-Wallis test followed by a Dunn's multiple comparison test for nonparametric data. All statistical calculations were performed using GraphPad Prism v5.0.

RESULTS

LCAT expression and activity in plasma is not affected by aging or the onset of amyloid pathology in APP/PS1 mice

As there has been a single report of decreased CSF LCAT activity in human AD subjects (42), we first determined whether age and/or the presence of Aβ deposits impacts LCAT expression or activity in APP/PS1 mice. As amyloid deposition and behavioral deficits have been reported to start between 6 and 8 months of age in this line, we analyzed male APP/PS1 mice at 5 months of age, prior to disease onset, at 11 months of age, where mice demonstrate moderate pathology, and at 15.5 months of age, the age of the mice used in this study when pathology is very pronounced. Neither liver nor cortical LCAT mRNA was significantly changed with age (**Fig. 1A**). We next measured the total circulating levels of plasma LCAT and apoA-I, which is the major physiological activator of LCAT in plasma. There was a significant 27% increase in plasma LCAT levels and a nonsignificant 36% increase of plasma apoA-I in 15.5-month-old APP/PS1 mice compared with 5-month-old APP/PS1 mice (Fig. 1B, C). However, plasma LCAT activity, measured directly using artificial liposome substrates ex vivo (Fig. 1D) and measured indirectly by quantifying the relative abundance of plasma

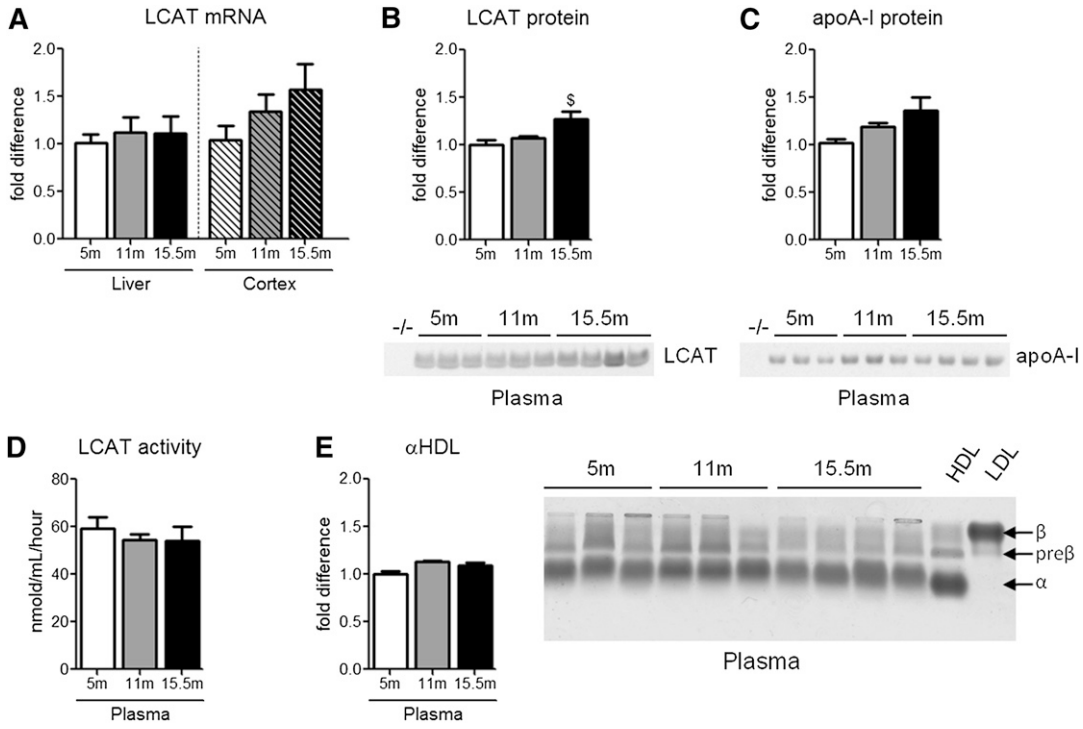

Fig. 1. Expression, levels, and plasma activity of LCAT are unaffected by age or the accumulation of Aβ and amyloid. LCAT mRNA, protein levels, and activity in addition to plasma apoA-I levels were measured in 5-, 11-, and 15.5-month-old male APP/PS1 mice. Plasma from young $LCAT^{-/-}$ mice, denoted as simply −/−, was used as a reference control. LCAT mRNA in the liver and cortex of APP/PS1 mice was measured by qRT-PCR (A). B: Plasma LCAT protein levels were measured by denaturing immunoblotting. C: Plasma levels of apoA-I were measured by denaturing immunoblotting. D: The activity of plasma LCAT was measured by determining the coefficient of esterification, defined by the ratio of CE/FC, following incubation of plasma with ^{3}H-cholesterol-labeled liposomes. E: Plasma αHDL levels were quantified as a secondary measure of LCAT activity. Plasma samples were subjected to native gel electrophoresis through Sebia gels and stained with Sudan black, which binds to lipids. Purified human HDL and LDL were run for comparison. Graphs represent mean ± SEM with N = 3–10 per group. Data were analyzed using a Kruskal-Wallis test followed by a Dunn's multiple comparison test.

α-migrating HDL (Fig. 1E), was unaffected by age or the onset of amyloid deposition. Although it would have been ideal to measure LCAT activity in the CSF of these animals, these experiments were not feasible due to the low yield of CSF and dilute LCAT levels in CSF.

LCAT deficiency selectively reduces plasma and CNS apoA-I

Next, we analyzed plasma lipoprotein levels and distribution following total body deletion of LCAT from male APP/PS1 mice. As expected, plasma apoA-I and total HDL-C were dramatically reduced to 14% and 8% of APP/PS1 WT littermate control levels (**Fig. 2A, B**). Plasma lipoprotein subspecies were further characterized by separating whole plasma using Sebia gels, which separate lipoprotein particles based on surface charge, followed by Sudan black staining to detect lipids. As expected, deletion of LCAT from APP/PS1 mice results in an almost complete absence of mature α-migrating HDL and an enrichment of lipoproproteins at the gel origin, which most likely includes chylomicrons (43) (Fig. 2C). These results are consistent with previous characterization of young male LCAT$^{-/-}$ mice on a C57Bl.6 background (45), indicating that advanced age and the onset of amyloid pathology does not influence the robust plasma lipoprotein phenotype induced by LCAT deficiency.

We then assessed the impact of LCAT deficiency on the levels of apoA-I- and apoE-containing lipoprotein particles in the CNS. While apoA-I is considered the major physiological activator of LCAT in the plasma (43), this role is believed to be filled by apoE in the CNS (47). In parallel to the observations in plasma, the level of apoA-I in the cortex, hippocampus, and CSF of APP/PS1 LCAT$^{-/-}$ mice was reduced to 30% ($P < 0.0001$), 10% ($P = 0.0571$), and 11% of APP/PS1 WT littermate controls (**Fig. 3A**). Conversely, loss of LCAT did not affect apoE levels in either brain tissue or CSF (Fig. 3B). Further, the size and distribution of apoE-containing lipoprotein particles in CSF were similar between APP/PS1 WT and APP/PS1 LCAT$^{-/-}$ mice (supplementary Fig. I). Lastly, we investigated whether LCAT deficiency impacts CNS expression of key receptors involved in cholesterol and lipoprotein metabolism, namely ABCA1, LDLR, LRP1, and scavenger receptor BI (SR-BI) (supplementary Fig. II). The absence of LCAT has no effect on cortical and hippocampal levels of ABCA1 and LRP1 (supplementary Fig. IIA, C), but was associated with a 40% increase in hippocampal LDLR levels (supplementary Fig. IIB; $P = 0.0317$) and a 71% decrease in hippocampal scavenger receptor BI (supplementary Fig. 2D; $P = 0.0357$).

Aβ and amyloid deposition are not increased by loss of LCAT in APP/PS1 mice

If LCAT-mediated lipoprotein maturation is required for efficient Aβ clearance, LCAT deficiency would be expected to elevate Aβ levels and amyloid burden in vivo. We observed no consistent and significant changes in either soluble or aggregated Aβ levels and in total or vascular amyloid burden (**Figs. 4, 5**). In contrast to the expected observation of increased Aβ levels, we were surprised to find a 46% decrease ($P = 0.0173$) in cortical levels of carbonate soluble Aβ42 in APP/PS1 LCAT$^{-/-}$ mice, albeit this was the only significant change detected for Aβ levels (Fig. 4). Notably, the ratio of Aβ40:Aβ42 was increased by 70% in carbonate and guanidine soluble cortical lysates ($P = 0.0357$ carbonate soluble, $P = 0.1181$ GuHCl soluble) and by 130% in guanidine soluble hippocampal lysates ($P = 0.0087$). Histological analysis using thioflavin-A, which detects total amyloid, and resorufin staining, which specifically binds to vascular amyloid (54), revealed no change in total or cerebrovascular amyloid burden between APP/PS1 WT and APP/PS1 LCAT$^{-/-}$ mice (Fig. 5).

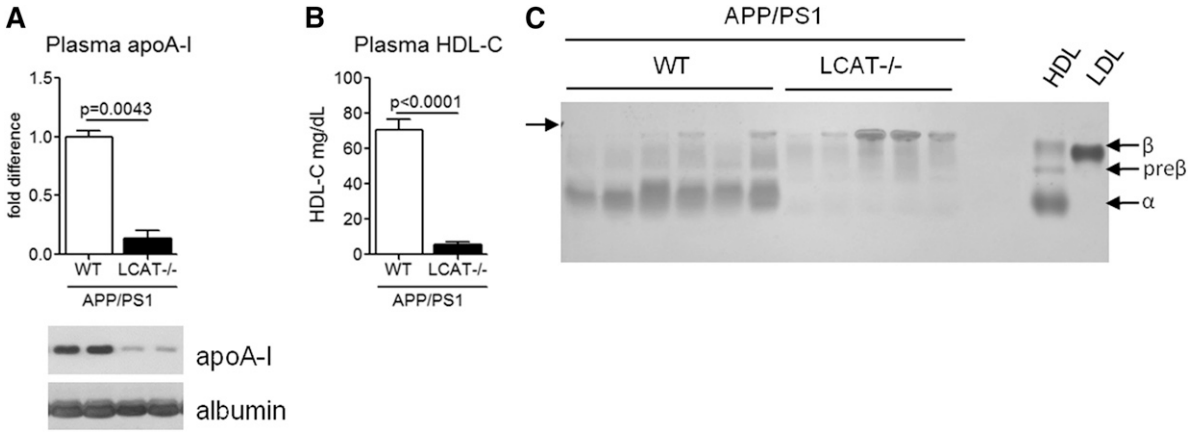

Fig. 2. Deletion of LCAT in APP/PS1 mice significantly reduces HDL-C, specifically α-migrating particles. A: Plasma apoA-I protein levels were measured by denaturing immunoblotting. B: Total plasma HDL-C was measured using a commercial enzymatic kit. C: Plasma samples were subjected to native gel electrophoresis through Sebia gels and stained with Sudan black, which binds to lipids. Purified human HDL and LDL were run for comparison. Graphs represent mean ± SEM with N = 5–6 per group. Data were analyzed using Mann-Whitney test (A) and Student's unpaired *t*-test (B).

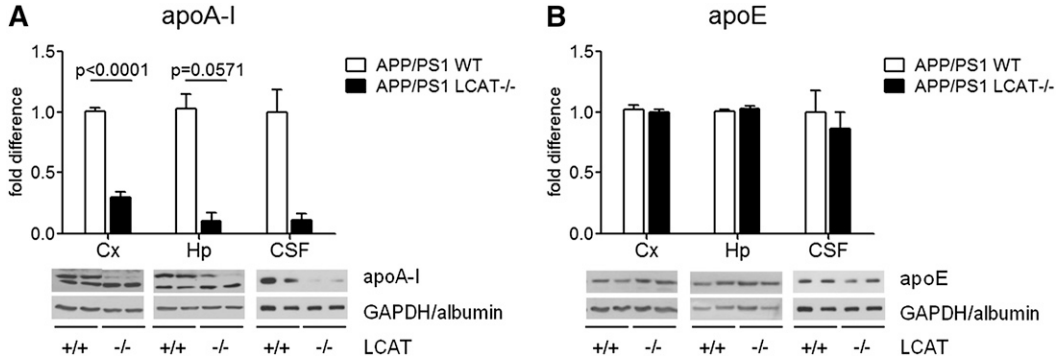

Fig. 3. CNS apoA-I is significantly reduced in APP/PS1 LCAT$^{-/-}$ mice. Protein levels of apoA-I (A) and apoE (B) were measured by denaturing immunoblotting in cortical (far left) and hippocampal (center) lysates in addition to CSF (far right). Values are expressed for each region compared with APP/PS1 WT controls. Graphs represent mean ± SEM with N = 3–6 per group, except for CSF where N = 2 per group. Data were analyzed using a Student's unpaired *t*-test (cortical apoA-I) or Mann Whitney test (hippocampal apoA-I).

DISCUSSION

Although LCAT is well-characterized with respect to its impact on peripheral HDL metabolism (43), little is known about its function in the CNS. While the initial lipidation of glial-derived apoE by ABCA1 is a critical determinant in its ability to mediate Aβ degradation and clearance (32, 33, 35), it is unknown whether the generation of the CE core by LCAT is also required. Our data show that total body deletion of LCAT, which blocks HDL lipoprotein maturation, does not significantly impair Aβ or amyloid deposition in APP/PS1 mice (Fig. 4, 5). This finding provides strong support for the hypothesis that Aβ clearance is mediated by nascent discoidal lipoprotein particles (whether apoA-I or apoE derived) rather than mature spherical plasma or CNS lipoproteins. As APP/PS1 mice develop vascular amyloid deposits much later than parenchymal deposits, we specifically designed our study to investigate Aβ and amyloid load at 15.5 months of age, when both total and vascular deposits are robust. However, we cannot rule out the possibility that LCAT deficiency may have altered the age of onset of Aβ or amyloid deposition.

It is also important to note that both apoE and apoA-I lipoproteins may affect Aβ and amyloid metabolism. Lefterov et al. (55) previously reported a robust and specific increase of cerebrovascular amyloid angiopathy in 12-month-old APP/PS1 mice that were crossed onto a total apoA-I knockout background, suggesting that apoA-I specifically affects vascular amyloid levels. We observed no change in vascular amyloid burden in APP/PS1 LCAT$^{-/-}$ mice (Fig. 5F), despite a 70–90% reduction in plasma and CNS apoA-I (Figs. 2A, 3A). However, LCAT-deficient mice are not equivalent to apoA-I-deficient mice, as approximately 10% of apoA-I remains in the absence of LCAT and much of this apoA-I is believed to be in the preβ form (44, 45). It is therefore possible that preβ apoA-I HDL is more important or more efficient than α-HDL with respect to amyloid clearance within the cerebrovasculature. Although not specifically measured in our study, there have been previous reports of increased plasma preβ HDL in LCAT-deficient mice (44, 45) and in human subjects with

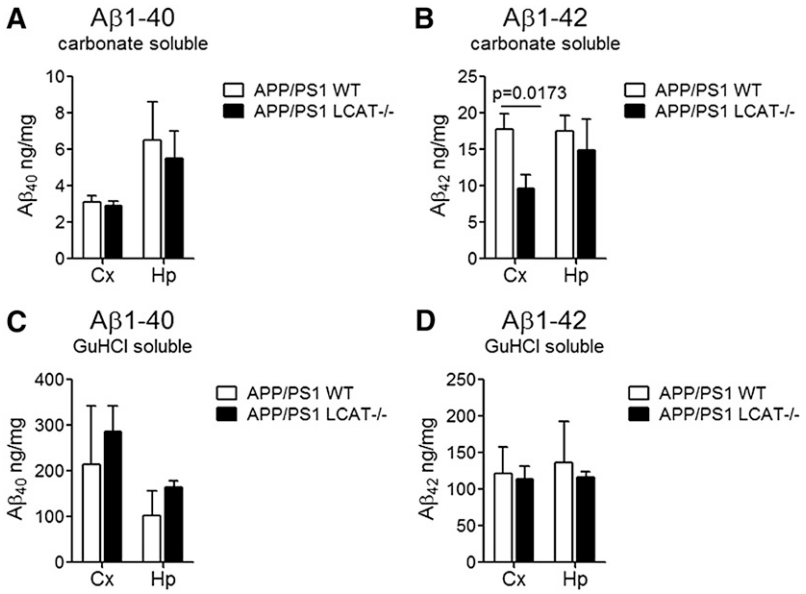

Fig. 4. Loss of LCAT does not have a substantial effect on levels of soluble or insoluble Aβ40 or Aβ42 in the cortex or hippocampus. Levels of carbonate soluble Aβ40 (A) Aβ42 (B), and GuHCl soluble Aβ40 (C) and Aβ42 (D) were measured by commercial ELISA. Graphs represent mean ± SEM with N = 5–6 per group. Data were analyzed using a Mann Whitney test.

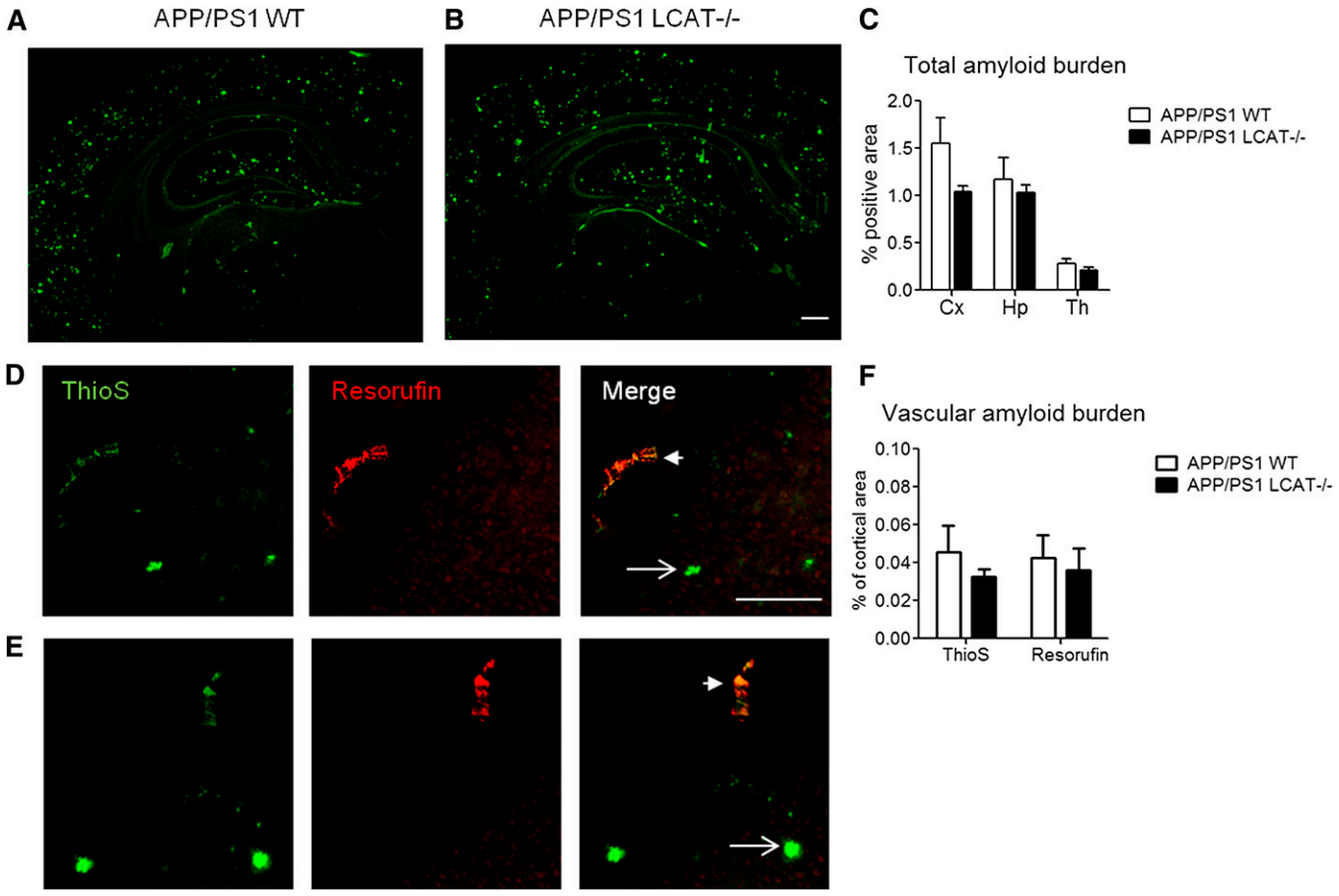

Fig. 5. Parenchymal and vascular amyloid deposition is independent of LCAT in APP/PS1 mice. Representative images taken at 100× magnification of coronal half brain sections from APP/PS1 WT (A) and APP/PS1 LCAT$^{-/-}$ (B) stained with thioflavin S (ThioS) to visualize total amyloid deposition. Scale bar represents 2 mM. C: Amyloid burden is expressed as percent of total area measured, in the cortex (Cx), hippocampus (Hp), and thalamus (Th). Graphs represent mean ± SEM with N = 4–5 per group and four to five sections per mouse. A subset of sections was further costained with thioflavin S (green) and resorufin (red), which binds only to vascular amyloid. Representative images taken at 100× magnification of coronal half brain sections from APP/PS1 WT (D) and APP/PS1 LCAT$^{-/-}$ (E) showing parenchymal (arrow) and vascular (arrowhead) amyloid deposition in the cortex. Scale bar represents 200 μM. F: Quantification of vascular amyloid burden in the cortex expressed as percent of cortical area using either thioflavin S or resorufin. Graph represents mean ± SEM with N = 3–6 per group and two to four sections per mouse.

mutant LCAT alleles resulting in increased ABCA1-mediated cholesterol efflux (56). In contrast to apoA-I, the electrophoretic mobility characteristics of nascent discoidal apoE particles is not known.

Another finding of this study is that neither age nor the presence of amyloid deposits affects LCAT expression in the liver and cortex, or more importantly, plasma LCAT activity in the APP/PS1 mouse model (Fig. 1). In contrast, a 50% decrease in CSF LCAT activity in human AD subjects compared with age-matched nondemented controls has been previously reported (42). Although it would be ideal to measure LCAT activity in the CSF of APP/PS1 mice, the small volume of CSF (approximately 10 μl per mouse) obtained from mice and predicted LCAT levels and activity (2.5% of that in serum) pose significant challenges to this experiment (42). Future studies will be needed to determine if CSF LCAT levels are consistently reduced in AD subjects and, if so, whether this is correlated with other AD-relevant CSF biomarker changes, including Aβ and tau. As APP/PS1 mice do not develop neurofibrillary tangles or marked neurodegeneration, they may not model all of the components of AD pathology that may act in concert to suppress LCAT activity in human CSF.

Although LCAT deficiency does not impair Aβ metabolism in APP/PS1 mice, it is important to recognize that LCAT may have other important functions with respect to CNS lipoprotein metabolism. Lipoprotein maturation is a key step in lipoprotein-mediated transfer of lipids from one tissue source to another through body fluids. As apoE-containing lipoproteins are the major source by which adult neurons acquire the lipids necessary for the maintenance and repair of membranes, it is possible that the impact of LCAT deficiency may be most evident when apoE is required for lipid transport, such as under acute conditions of neuronal damage. Traumatic brain injury in humans, for example, leads to a significant decrease in CSF apoE levels but not of CSF apoA-I levels (57), and loss of apoE impairs recovery after traumatic brain injury in mice (58). Future studies may reveal a role for CNS LCAT to facilitate lipid transport in response to acute neuronal damage.

The authors are indebted to Dr. John Parks for providing the LCAT$^{-/-}$ mice used in this study

REFERENCES

1. Verghese, P. B., J. M. Castellano, and D. M. Holtzman. 2011. Apolipoprotein E in Alzheimer's disease and other neurological disorders. *Lancet Neurol.* **10:** 241–252.
2. Corder, E. H., A. M. Saunders, W. J. Strittmatter, D. E. Schmechel, P. C. Gaskell, G. W. Small, A. D. Roses, J. L. Haines, and M. A. Pericak-Vance. 1993. Gene dose of apolipoprotein E type 4 allele and the risk of Alzheimer's disease in late onset families. *Science.* **261:** 921–923.
3. Stukas, S., J. Robert, and C. L. Wellington. 2014. High density lipoproteins and cerebrovasular integrity in Alzheimer's disease. *Cell Metab.* **19:** 574–591.
4. Strittmatter, W. J., A. M. Saunders, D. Schmechel, M. Pericak-Vance, J. Enghild, G. S. Salvesen, and A. D. Roses. 1993. Apolipoprotein E: high-avidity binding to beta-amyloid and increased frequency of type 4 allele in late-onset familial Alzheimer disease. *Proc. Natl. Acad. Sci. USA.* **90:** 1977–1981.
5. Schmechel, D. E., A. M. Saunders, W. J. Strittmatter, B. J. Crain, C. M. Hulette, S. H. Joo, M. A. Pericak-Vance, D. Goldgaber, and A. D. Roses. 1993. Increased amyloid beta-peptide deposition in cerebral cortex as a consequence of apolipoprotein E genotype in late-onset Alzheimer disease. *Proc. Natl. Acad. Sci. USA.* **90:** 9649–9653.
6. Polvikoski, T., R. Sulkava, M. Haltia, K. Kainulainen, A. Vuorio, A. Verkkoniemi, L. Niinisto, P. Halonen, and K. Kontula. 1995. Apolipoprotein E, dementia, and cortical deposition of beta-amyloid protein. *N. Engl. J. Med.* **333:** 1242–1247.
7. Holtzman, D. M., A. M. Fagan, B. Mackey, T. Tenkova, L. Sartorius, S. M. Paul, K. Bales, K. H. Ashe, M. C. Irizarry, and B. T. Hyman. 2000. Apolipoprotein E facilitates neuritic and cerebrovascular plaque formation in an Alzheimer's disease model. *Ann. Neurol.* **47:** 739–747.
8. Irizarry, M. C., G. W. Rebeck, B. Cheung, K. Bales, S. M. Paul, D. Holzman, and B. T. Hyman. 2000. Modulation of A beta deposition in APP transgenic mice by an apolipoprotein E null background. *Ann. N. Y. Acad. Sci.* **920:** 171–178.
9. Bales, K. R., T. Verina, D. J. Cummins, Y. Du, R. C. Dodel, J. Saura, C. E. Fishman, C. A. DeLong, P. Piccardo, V. Petegnief, et al. 1999. Apolipoprotein E is essential for amyloid deposition in the APP(V717F) transgenic mouse model of Alzheimer's disease. *Proc. Natl. Acad. Sci. USA.* **96:** 15233–15238.
10. Bales, K. R., T. Verina, R. C. Dodel, Y. Du, L. Altstiel, M. Bender, P. Hyslop, E. M. Johnstone, S. P. Little, D. J. Cummins, et al. 1997. Lack of apolipoprotein E dramatically reduces amyloid beta-peptide deposition. *Nat. Genet.* **17:** 263–264.
11. Fryer, J. D., J. W. Taylor, R. B. DeMattos, K. R. Bales, S. M. Paul, M. Parsadanian, and D. M. Holtzman. 2003. Apolipoprotein E markedly facilitates age-dependent cerebral amyloid angiopathy and spontaneous hemorrhage in amyloid precursor protein transgenic mice. *J. Neurosci.* **23:** 7889–7896.
12. Holtzman, D. M., K. R. Bales, T. Tenkova, A. M. Fagan, M. Parsadanian, L. J. Sartorius, B. Mackey, J. Olney, D. McKeel, D. Wozniak, et al. 2000. Apolipoprotein E isoform-dependent amyloid deposition and neuritic degeneration in a mouse model of Alzheimer's disease. *Proc. Natl. Acad. Sci. USA.* **97:** 2892–2897.
13. Fagan, A. M., M. Watson, M. Parsadanian, K. R. Bales, S. M. Paul, and D. M. Holtzman. 2002. Human and murine ApoE markedly alters A beta metabolism before and after plaque formation in a mouse model of Alzheimer's disease. *Neurobiol. Dis.* **9:** 305–318.
14. Fryer, J. D., K. Simmons, M. Parsadanian, K. R. Bales, S. M. Paul,, P. M. Sullivan, and D. M. Holtzman. 2005. Human apolipoprotein E4 alters the amyloid-beta 40:42 ratio and promotes the formation of cerebral amyloid angiopathy in an amyloid precursor protein transgenic model. *J. Neurosci.* **25:** 2803–2810.
15. Bales, K. R., F. Liu, S. Wu, S. Lin, D. Koger, C. DeLong, J. C. Hansen, P. M. Sullivan, and S. M. Paul. 2009. Human APOE isoform-dependent effects on brain β-amyloid levels in PDAPP transgenic mice. *J. Neurosci.* **29:** 6771–6779.
16. Castellano, J. M., J. Kim, F. R. Stewart, H. Jiang, R. B. DeMattos, B. W. Patterson, A. M. Fagan, J. C. Morris, K. G. Mawuenyega, C. Cruchaga, et al. 2011. Human apoE isoforms differentially regulate brain amyloid-β peptide clearance. *Sci. Transl. Med.* **3:** 89ra57.
17. Kim, J., H. Jiang, S. Park, A. E. Eltorai, F. R. Stewart, H. Yoon, J. M. Basak, M. B. Finn, and D. M. Holtzman. 2011. Haploinsufficiency of human APOE reduces amyloid deposition in a mouse model of amyloid-β amyloidosis. *J. Neurosci.* **31:** 18007–18012.
18. Sagare, A. P., R. D. Bell, and B. V. Zlokovic. 2012. Neurovascular dysfunction and faulty amyloid β-peptide clearance in Alzheimer disease. *Cold Spring Harb. Perspect. Med.* **2:** a011452.
19. Saido, T., and M. A. Leissring. 2012. Proteolytic degradation of amyloid β-protein. *Cold Spring Harb. Perspect. Med.* **2:** a006379.
20. Deane, R., A. Sagare, K. Hamm, M. Parisi, S. Lane, M. B. Finn, D. M. Holtzman, and B. V. Zlokovic. 2008. apoE isoform-specific disruption of amyloid beta peptide clearance from mouse brain. *J. Clin. Invest.* **118:** 4002–4013.
21. Bell, R. D., A. P. Sagare, A. E. Friedman, G. S. Bedi, D. M. Holtzman, R. Deane, and B. V. Zlokovic. 2007. Transport pathways for clearance of human Alzheimer's amyloid beta-peptide and apolipoproteins E and J in the mouse central nervous system. *J. Cereb. Blood Flow Metab.* **27:** 909–918.
22. Bien-Ly, N., A. K. Gillespie, D. Walker, S. Y. Yoon, and Y. Huang. 2012. Reducing human apolipoprotein E levels attenuates age-dependent Aβ accumulation in mutant human amyloid precursor protein transgenic mice. *J. Neurosci.* **32:** 4803–4811.
23. Verghese, P. B., J. M. Castellano, K. Garai, Y. Wang, H. Jiang, A. Shah, G. Bu, C. Frieden, and D. M. Holtzman. 2013. ApoE influences amyloid-β (Aβ) clearance despite minimal apoE/Aβ association in physiological conditions. *Proc. Natl. Acad. Sci. USA.* **110:** E1807–E1816.
24. Tai, L. M., T. Bilousova, L. Jungbauer, S. K. Roeske, K. L. Youmans, C. Yu, W. W. Poon, L. B. Cornwell, C. A. Miller, H. V. Vinters, et al. 2013. Levels of soluble apolipoprotein E/amyloid-β (Aβ) complex are reduced and oligomeric Aβ increased with APOE4 and Alzheimer disease in a transgenic mouse model and human samples. *J. Biol. Chem.* **288:** 5914–5926.
25. Fryer, J. D., R. B. Demattos, L. M. McCormick, M. A. O'Dell, M. L. Spinner, K. R. Bales, S. M. Paul, P. M. Sullivan, M. Parsadanian, G. Bu, et al. 2005. The low density lipoprotein receptor regulates the level of central nervous system human and murine apolipoprotein E but does not modify amyloid plaque pathology in PDAPP mice. *J. Biol. Chem.* **280:** 25754–25759.
26. Castellano, J. M., R. Deane, A. J. Gottesdiener, P. B. Verghese, F. R. Stewart, T. West, A. C. Paoletti, T. R. Kasper, R. B. DeMattos, B. V. Zlokovic, et al. 2012. Low-density lipoprotein receptor overexpression enhances the rate of brain-to-blood Aβ clearance in a mouse model of β-amyloidosis. *Proc. Natl. Acad. Sci. USA.* **109:** 15502–15507.
27. Johnson, L. A., R. H. Olsen, L. S. Merkens, A. DeBarber, R. D. Steiner, P. M. Sullivan, N. Maeda, and J. Raber. 2014. Apolipoprotein E-low density lipoprotein receptor interaction affects spatial memory retention and brain ApoE levels in an isoform-dependent manner. *Neurobiol. Dis.* **64:** 150–162.
28. Hirsch-Reinshagen, V., S. Zhou, B. L. Burgess, L. Bernier, S. A. McIsaac, J. Y. Chan, G. H. Tansley, J. S. Cohn, M. R. Hayden, and C. L. Wellington. 2004. Deficiency of ABCA1 impairs apolipoprotein E metabolism in brain. *J. Biol. Chem.* **279:** 41197–41207.
29. Wahrle, S. E., H. Jiang, M. Parsadanian, J. Legleiter, X. Han, J. D. Fryer, T. Kowalewski, and D. M. Holtzman. 2004. ABCA1 is required for normal central nervous system ApoE levels and for lipidation of astrocyte-secreted apoE. *J. Biol. Chem.* **279:** 40987–40993.
30. Koldamova, R., N. F. Fitz, and I. Lefterov. ATP-binding cassette transporter A1: from metabolism to neurodegeneration. *Neurobiol. Dis.* Epub ahead of print. May 17, 2014; doi:10.1016/j.nbd.2014,05,007.
31. Aiello, R. J., D. Brees, and O. L. Francone. 2003. ABCA1-deficient mice: insights into the role of monocyte lipid efflux in HDL formation and inflammation. *Arterioscler. Thromb. Vasc. Biol.* **23:** 972–980.
32. Hirsch-Reinshagen, V., L. F. Maia, B. L. Burgess, J. F. Blain, K. E. Naus, S. A. McIsaac, P. F. Parkinson, J. Y. Chan, G. H. Tansley, M. R. Hayden, et al. 2005. The absence of ABCA1 decreases soluble ApoE levels but does not diminish amyloid deposition in two murine models of Alzheimer disease. *J. Biol. Chem.* **280:** 43243–43256.
33. Koldamova, R., M. Staufenbiel, and I. Lefterov. 2005. Lack of ABCA1 considerably decreases brain ApoE level and increases amyloid deposition in APP23 mice. *J. Biol. Chem.* **280:** 43224–43235.
34. Wahrle, S. E., H. Jiang, M. Parsadanian, R. E. Hartman, K. R. Bales, S. M. Paul, and D. M. Holtzman. 2005. Deletion of Abca1 increases Abeta deposition in the PDAPP transgenic mouse model of Alzheimer disease. *J. Biol. Chem.* **280:** 43236–43242.

35. Wahrle, S. E., H. Jiang, M. Parsadanian, J. Kim, A. Li, A. Knoten, S. Jain, V. Hirsch-Reinshagen, C. L. Wellington, K. R. Bales, et al. 2008. Overexpression of ABCA1 reduces amyloid deposition in the PDAPP mouse model of Alzheimer disease. *J. Clin. Invest.* **118:** 671–682.
36. Fan, J., S. Stukas, C. Wong, J. Chan, S. May, N. DeValle, V. Hirsch-Reinshagen, A. Wilkinson, M. N. Oda, and C. L. Wellington. 2011. An ABCA1-independent pathway for recycling a poorly lipidated 8.1 nm apolipoprotein E particle from glia. *J. Lipid Res.* **52:** 1605–1616.
37. DeMattos, R. B., R. P. Brendza, J. E. Heuser, M. Kierson, J. R. Cirrito, J. Fryer, P. M. Sullivan, A. M. Fagan, X. Han, and D. M. Holtzman. 2001. Purification and characterization of astrocyte-secreted apolipoprotein E and J-containing lipoproteins from wild-type and human apoE transgenic mice. *Neurochem. Int.* **39:** 415–425.
38. LaDu, M. J., S. M. Gilligan, J. R. Lukens, V. G. Cabana, C. A. Reardon, L. J. Van Eldik, and D. M. Holtzman. 1998. Nascent astrocyte particles differ from lipoproteins in CSF. *J. Neurochem.* **70:** 2070–2081.
39. Fagan, A. M., D. M. Holtzman, G. Munson, T. Mathur, D. Schneider, L. K. Chang, G. S. Getz, C. A. Reardon, J. Lukens, J. A. Shah, et al. 1999. Unique lipoproteins secreted by primary astrocytes from wild type, apoE (-/-), and human apoE transgenic mice. *J. Biol. Chem.* **274:** 30001–30007.
40. Pitas, R. E., J. K. Boyles, S. H. Lee, D. Hui, and K. H. Weisgraber. 1987. Lipoproteins and their receptors in the central nervous system. Characterization of the lipoproteins in cerebrospinal fluid and identification of apolipoprotein B,E(LDL) receptors in the brain. *J. Biol. Chem.* **262:** 14352–14360.
41. Koch, S., N. Donarski, K. Goetze, M. Kreckel, H. J. Stuerenburg, C. Buhmann, and U. Beisiegel. 2001. Characterization of four lipoprotein classes in human cerebrospinal fluid. *J. Lipid Res.* **42:** 1143–1151.
42. Demeester, N., G. Castro, C. Desrumaux, C. De Geitere, J. C. Fruchart, P. Santens, E. Mulleners, S. Engelborghs, P. P. De Deyn, J. Vandekerckhove, et al. 2000. Characterization and functional studies of lipoproteins, lipid transfer proteins, and lecithin:cholesterol acyltransferase in CSF of normal individuals and patients with Alzheimer's disease. *J. Lipid Res.* **41:** 963–974.
43. Rousset, X., R. Shamburek, B. Vaisman, M. Amar, and A. T. Remaley. 2011. Lecithin cholesterol acyltransferase: an anti- or pro-atherogenic factor? *Curr. Atheroscler. Rep.* **13:** 249–256.
44. Ng, D. S., O. L. Francone, T. M. Forte, J. Zhang, M. Haghpassand, and E. M. Rubin. 1997. Disruption of the murine lecithin:cholesterol acyltransferase gene causes impairment of adrenal lipid delivery and up-regulation of scavenger receptor class B type I. *J. Biol. Chem.* **272:** 15777–15781.
45. Sakai, N., B. L. Vaisman, C. A. Koch, R. F. Hoyt, Jr., S. M. Meyn, G. D. Talley, J. A. Paiz, H. B. Brewer, Jr., and S. Santamarina-Fojo. 1997. Targeted disruption of the mouse lecithin:cholesterol acyltransferase (LCAT) gene. Generation of a new animal model for human LCAT deficiency. *J. Biol. Chem.* **272:** 7506–7510.
46. Tanigawa, H., J. T. Billheimer, J. Tohyama, I. V. Fuki, D. S. Ng, G. H. Rothblat, and D. J. Rader. 2009. Lecithin: cholesterol acyltransferase expression has minimal effects on macrophage reverse cholesterol transport in vivo. *Circulation.* **120:** 160–169.
47. Hirsch-Reinshagen, V., J. Donkin, S. Stukas, J. Chan, A. Wilkinson, J. Fan, J. S. Parks, J. A. Kuivenhoven, D. Lutjohann, H. Pritchard, et al. 2009. LCAT synthesized by primary astrocytes esterifies cholesterol on glia-derived lipoproteins. *J. Lipid Res.* **50:** 885–893.
48. Albers, J. J., S. M. Marcovina, and R. H. Christenson. 1992. Lecithin cholesterol acyltransferase in human cerebrospinal fluid: reduced level in patients with multiple sclerosis and evidence of direct synthesis in the brain. *Int. J. Clin. Lab. Res.* **22:** 169–172.
49. DeMattos, R. B., K. R. Bales, M. Parsadanian, M. A. O'Dell, E. M. Foss, S. M. Paul, and D. M. Holtzman. 2002. Plaque-associated disruption of CSF and plasma amyloid-beta (Abeta) equilibrium in a mouse model of Alzheimer's disease. *J. Neurochem.* **81:** 229–236.
50. Vaisman, B. L., H. G. Klein, M. Rouis, A. M. Berard, M. R. Kindt, G. D. Talley, S. M. Meyn, R. F. Hoyt, Jr., S. M. Marcovina, J. J. Albers, et al. 1995. Overexpression of human lecithin cholesterol acyltransferase leads to hyperalphalipoproteinemia in transgenic mice. *J. Biol. Chem.* **270:** 12269–12275.
51. Vaisman, B. L., and A. T. Remaley. 2013. Measurement of lecithin-cholesterol acyltransferase activity with the use of a Peptide-proteoliposome substrate. *Methods Mol. Biol.* **1027:** 343–352.
52. Yesilaltay, A., M. G. Morales, L. Amigo, S. Zanlungo, A. Rigotti, S. L. Karackattu, M. H. Donahee, K. F. Kozarsky, and M. Krieger. 2006. Effects of hepatic expression of the high-density lipoprotein receptor SR-BI on lipoprotein metabolism and female fertility. *Endocrinology.* **147:** 1577–1588.
53. Freeman, L. A. 2013. Western blots. *Methods Mol. Biol.* **1027:** 369–385.
54. Han, B. H., M. L. Zhou, A. K. Vellimana, E. Milner, D. H. Kim, J. K. Greenberg, W. Chu, R. H. Mach, and G. J. Zipfel. 2011. Resorufin analogs preferentially bind cerebrovascular amyloid: potential use as imaging ligands for cerebral amyloid angiopathy. *Mol. Neurodegener.* **6:** 86.
55. Lefterov, I., N. F. Fitz, A. A. Cronican, A. Fogg, P. Lefterov, R. Kodali, R. Wetzel, and R. Koldamova. 2010. Apolipoprotein A-I deficiency increases cerebral amyloid angiopathy and cognitive deficits in APP/PS1DeltaE9 mice. *J. Biol. Chem.* **285:** 36945–36957.
56. Calabresi, L., E. Favari, E. Moleri, M. P. Adorni, M. Pedrelli, S. Costa, W. Jessup, I. C. Gelissen, P. T. Kovanen, F. Bernini, et al. 2009. Functional LCAT is not required for macrophage cholesterol efflux to human serum. *Atherosclerosis.* **204:** 141–146.
57. Kay, A. D., S. P. Day, M. Kerr, J. A. Nicoll, C. J. Packard, and M. J. Caslake. 2003. Remodeling of cerebrospinal fluid lipoprotein particles after human traumatic brain injury. *J. Neurotrauma.* **20:** 717–723.
58. Namjoshi, D. R., G. Martin, J. Donkin, A. Wilkinson, S. Stukas, J. Fan, M. Carr, S. Tabarestani, K. Wuerth, R. E. Hancock, et al. 2013. The liver X receptor agonist GW3965 improves recovery from mild repetitive traumatic brain injury in mice partly through apolipoprotein E. *PLoS ONE.* **8:** e53529.